Supporting Information

Synergistic Optimization of Thermoelectric Performance in Polycrystalline and Crystalline SnS via Na Doping and Se Alloying

Shan Liu[1], Shulin Bai[1], Yi Wen[1], Bingchao Qin[1], Yixuan Hu[1], Tian Gao[1], Yichen Li[1], Lei Wang[1], Cheng Chang[1*], Li-Dong Zhao[1,2*]

[1]*School of Materials Science and Engineering, Beihang University, Beijing, 100191, China*

[2]*Tianmushan Laboratory, Beihang University, Hangzhou 311115, China.*

Corresponding authors: changchengcc@buaa.edu.cn; zhaolidong@buaa.edu.cn

Experimental Details

Raw materials:

Tin particles (Sn, Aladdin, 99.999%), Sulfur powders (S, Aladdin, 99.999%), Selenium particles (Se, Aladdin, 99.999%), Na blocks (99.95%).

Material synthesis:

High-purity Sn, S, and Se raw materials were weighed using an analytical balance in in an N_2-filled glove box, following the stoichiometric ratio of $Sn_{1-x}Na_xS$ (x = 0, 0.01, 0.02, 0.03, and 0.04) and $Sn_{0.98}Na_{0.02}S_{1-y}Se_y$ (y = 0, 0.1, 0.2, 0.3, 0.4, and 0.45) samples. The weighed mixtures were transferred into quartz tubes, which were flame-sealed under a vacuum of $< 10^{-4}$ Pa.

For the synthesis of precursor ingots, the sealed quartz tubes were subjected to a stepwise heating process: first ramped to 873 K over 20 hours, and then held at this temperature for 20 hours. Subsequently, it was further heated to 1223 K over 20 hours, and maintained at 1223 K for 15 hours, followed by furnace cooling.

On one hand, for the preparation of polycrystalline ingots, the obtained ingots were first ground into powders with a particle size less than 200 mesh in a glove box and then sieved. These powders were densified via hot-pressing sintering (OTF-1700X-RHP4, China) under vacuum conditions: a rapid temperature rise to 823 K within 15 minutes, followed by the application of 50 MPa for 10 minutes, and the sample was cooled in the furnace before being demolded, thus yielding densified bulk samples with dimensions of ~Φ15 × 10 mm^3.

On the other hand, for crystal growth, the precursor ingots were first ground into powders in an N_2-filled glove box. The powders were loaded into conical quartz tubes with a carbon coating on the inner wall, which were vacuum-sealed and subsequently subjected to flame sealing treatment. The sealed tubes were placed in a vertical furnace equipped with a temperature gradient. The crystal growth process was carried out as follows: the polycrystalline powders were heated to 1313 K over 20 hours, held at 1313 K for 15 hours, and then cooled down to 1073 K at a rate of 1 K h^{-1}, followed by furnace cooling.

Structural characterization:

The phase composition and preferred orientation of the samples were characterized using X-ray diffraction (XRD) with a D/max 2200PC X-ray diffractometer (Rigaku, Japan), utilizing Cu Kα (λ = 1.5418 Å) radiation, operating at 40 kV and 200 mA, and equipped with a position-sensitive detector. The microstructure and elemental distribution were examined using a scanning electron microscope (SEM) model JSM7500 (JEOL, Tokyo, Japan) equipped with an energy dispersive spectrometer (EDS).

Electrical transport property measurements:

Rectangular samples of ~ 3 × 3 × 8 mm^3 were prepared from the obtained SnS polycrystals. Measurements of the Seebeck coefficient and electrical conductivity were performed using an Ulvac Riko ZEM-3, Japan instrument. In order to avoid potential sample evaporation, a boron nitride layer was coated onto the samples. Measurements were taken along the direction perpendicular to the sintering pressure across a temperature range from 300 K to 873 K, ensuring that measurement errors of the above parameters kept below 5%.

Hall measurements:

Rectangular samples with 6 × 6 × 0.5 mm^3 were prepared for Hall measurements. The Hall coefficient (R_H) was acquired using the Van der Paw technique under Hall measurement system (Lake Shore, 8400 Series, USA) with a reversible magnetic field of 1.0 T at room temperature. The Hall carrier concentration (n_H) was calculated using the equation $n_H = 1/(eR_H)$, and the Hall mobility (μ_H) was determined by $\mu_H = \sigma R_H$, where e represents electric charge, and σ is the electrical conductivity.

Bandgap measurements:

The optical diffuse reflectance spectra of the powder samples were acquired at 300 K using a UV-vis-NIR spectrophotometer (UV-3600 Plus, Japan) equipped with an integrating sphere (ISR-603) featuring a polytetrafluoroethylene (PTFE) coating. Finely ground sample powders were homogeneously mixed with analytical-grade barium sulfate ($BaSO_4$) and uniformly coated onto a sample holder. Reflectance data (R) obtained from the diffuse reflectance spectra were subsequently transformed into

absorption data via the Kubelka-Munk function: $\alpha/S = (1-R)^2/2R$, where R, α, and S represent the reflectance, absorption coefficient, and scattering coefficient, respectively. The optical bandgap energies of the samples were then determined from the Kubelka-Munk transformed data.

Thermal transport property measurements:

Circular wafers with a diameter of 6 mm and thickness of ~ 1 mm were prepared to measure the thermal transport properties along the direction perpendicular to the sintering pressure. To minimize testing errors, a thin layer of graphite was applied to the samples. Thermal conductivity (κ) was calculated using the equation $\kappa = D\rho C_p$, where thermal diffusivity (D) was measured using a Netzsch LFA457, Germany instrument utilizing the laser flash method. The sample density (ρ) was measured by mass-to-volume ratio, and heat capacity (C_p) was obtained from the Dulong-Petit law. The lattice thermal conductivity (κ_{lat}) was then derived by directly subtracting electronic thermal conductivity (κ_{ele}) from the total thermal conductivity (κ_{tot}). κ_{ele} can be calculated using the Lorenz number (L), electrical conductivity (σ), and absolute temperature (T), following the relation $\kappa_{ele} = L\sigma T$. The Lorenz number (L) can be obtained as[1]:

$$L = \left(\frac{k_B}{e}\right)^2 \left\{ \frac{(r+7/2)F_{r+5/2}(\eta)}{(r+3/2)F_{r+1/2}(\eta)} - \left[\frac{(r+5/2)F_{r+3/2}(\eta)}{(r+3/2)F_{r+1/2}(\eta)} \right]^2 \right\} \quad \text{(S1)}$$

where k_B is the Boltzmann constant, e is the electron charge, r is the scattering rate, and η refers to the reduced Fermi energy, which can be derived from the measured Seebeck coefficients with consideration of acoustic phonon dominated scattering (r = -1/2):

$$S = \frac{k_B}{e} \left[\frac{(r+5/2)F_{r+3/2}(\eta)}{(r+3/2)F_{r+1/2}(\eta)} - \eta \right] \quad \text{(S2)}$$

where $F_x(\eta)$ is Fermi integral that can be defined as:

$$F_x(\eta) = \int_0^\infty \frac{\varepsilon^x}{1+\exp(\varepsilon-\mu)} d\varepsilon \quad \text{(S3)}$$

The uncertainty in obtaining the thermal conductivity was estimated to be within 8%.

Theoretical calculation of lattice thermal conductivity by Callaway model:

According to the Callaway model, the ratio of κ_{lat} of the parent material compound

to that of the Se-alloyed material was expressed as the following formula[2-3]:

$$\frac{\kappa_{\text{lat}}}{\kappa_{\text{lat,p}}} = \frac{\tan^{-1}(u)}{u} \tag{S4}$$

where κ_{lat} and $\kappa_{\text{lat,p}}$ were lattice thermal conductivities of Se-alloyed material and parent material ($\kappa_{\text{lat,p}}$ = 1.63 W m^{-1} K^{-1}), respectively. The parameter u was defined as follow:

$$u = \left(\frac{\pi^2 \theta_D \Omega}{h v_a^2} \kappa_{\text{lat,p}} \Gamma \right)^{1/2} \tag{S5}$$

$$\theta_D = \frac{h}{k_B} \left(\frac{3}{4\pi\Omega} \right)^{1/3} v_a \tag{S6}$$

Here, Θ_{D}, Ω, h, v_{a}, Γ, respectively represented the Debye temperature, the average volume of each atom, the Planck constant, the average sound velocity, and the imperfection scaling parameter. The Γ consisted of two parts: the mass fluctuation (Γ_{M}) and the strain field fluctuation (Γ_{S}). The relationship among the three physical quantities was expressed by the following formula:

$$\Gamma = \Gamma_{\text{M}} + \varepsilon \Gamma_{\text{S}} \tag{S7}$$

Here, ε was a phenomenological adjustable parameter related to the Poisson ratio (v_{p}) and Grüneisen parameter (γ), and was expressed by[4]:

$$\varepsilon = \frac{2}{9} \left(\frac{6.4 \times \gamma (1 + v_{\text{p}})}{(1 - v_{\text{p}})} \right)^2 \tag{S8}$$

$$v_{\text{p}} = \frac{1 - 2(v_{\text{s}} / v_{\text{l}})^2}{2 - 2(v_{\text{s}} / v_{\text{l}})^2} \tag{S9}$$

$$\gamma = \frac{3}{2} \left(\frac{1 + v_{\text{p}}}{2 - 3v_{\text{p}}} \right) \tag{S10}$$

In $Sn_{0.98}Na_{0.02}S_{1-y}Se_y$ system, the sites of Sn and Na have not changed, therefore $\Gamma_{(\text{Sn, Ag})} = 0$, The $\Gamma_{Sn_{0.98}Ag_{0.02}S_{1-y}Se_y}$ was defined as follows:

$$\Gamma_{Sn_{0.98}Ag_{0.02}S_{1-y}Se_y} = \frac{1}{2} \left(\frac{M_{(\text{Sn,Ag})}}{\overline{M}} \right)^2 \Gamma_{(\text{Sn,Ag})} + \frac{1}{2} \left(\frac{M_{(\text{S,Se})}}{\overline{M}} \right)^2 \Gamma_{(\text{S,Se})} \tag{S11}$$

$$\Gamma_{(\text{S,Se})} = \Gamma_{\text{M(S,Se)}} + \varepsilon \Gamma_{\text{S(S,Se)}} \tag{S12}$$

$$\Gamma_{\mathrm{M(S,Se)}} = y(1-y)\left(\frac{\Delta M_{(\mathrm{S,Se})}}{M_{(\mathrm{S,Se})}}\right)^2 \tag{S13}$$

$$\Gamma_{\mathrm{S(S,Se)}} = y(1-y)\left(\frac{\Delta r_{(\mathrm{S,Se})}}{r_{(\mathrm{S,Se})}}\right)^2 \tag{S14}$$

$$\Delta M_{(\mathrm{S,Se})} = M_{\mathrm{S}} - M_{\mathrm{Se}} \tag{S15}$$

$$M_{(\mathrm{S,Se})} = (1-y)M_{\mathrm{S}} + yM_{\mathrm{Se}} \tag{S16}$$

$$\Delta r_{(\mathrm{S,Se})} = r_{\mathrm{S}} - r_{\mathrm{Se}} \tag{S17}$$

$$r_{(\mathrm{S,Se})} = (1-y)r_{\mathrm{S}} + yr_{\mathrm{Se}} \tag{S18}$$

Based on the above calculations, the Callaway-model-simulated κ_{lat} could be obtained.

Calculation for the heat capacity (C_{p}) based on the Debye model.

Based on the Debye model, the individual contributions of phonons and the effects of thermal expansion to the total heat capacity $C_{\mathrm{p,tot}}$ of the SnS system were considered. The total heat capacity, as a function of temperature, can be expressed as[5-6]:

$$C_{p,\,\mathrm{tot}}(T) = C_{p,ph}(T) + C_{p,D}(T) \tag{S19}$$

where $C_{\mathrm{p,ph}}$ and $C_{\mathrm{p,D}}$ represent the phonon heat capacity and the effects of lattice dilation on the heat capacity, respectively.

Here, due to the Debye assumption and elastic wave approximation, the phonon heat capacity can be obtained as:

$$C_{p,ph}\left(T/\Theta_D\right) = 9R\left(\frac{T}{\Theta_D}\right)^3 \int_0^{\Theta_D/T} \frac{x^4 e^x}{\left(e^x-1\right)^2} dx \tag{S20}$$

where R = 8.314 J mol^{-1} K^{-1}, and $x = \hbar\omega/k_{\mathrm{B}}T$, in which $\hbar$ and ω represent Planck constant (~6.626×10^{-34}) and phonon vibration frequency, respectively.

The effects of thermal expansion on the heat capacity can be derived from the thermal expansion in a given system. The effects of lattice dilation on the $C_{\mathrm{p,tot}}$, $C_{\mathrm{p,D}}$, can be obtained from:

$$C_{p,D}(T) = C_{ele,D}(T) + C_{ph,D}(T) = \frac{9BT\alpha^2}{10^6\rho} \tag{S21}$$

where a is the linear coefficient of thermal expansion, B is the isothermal bulk modulus, and ρ is the sample density. Based on the above discussion, $C_{p,tot}$ for all samples from Debye model can be obtained.

The calculation of the weighted mobility μ_w:

The μ_w is an inherent feature of material, which can be express as[7] :

$$\mu_W = \frac{3h^3\sigma}{8\pi e(2m_e k_B T)^{3/2}} \tag{S22}$$

Among them, m_e is the effective mass of electron (~9.109×10^{-31} Kg).

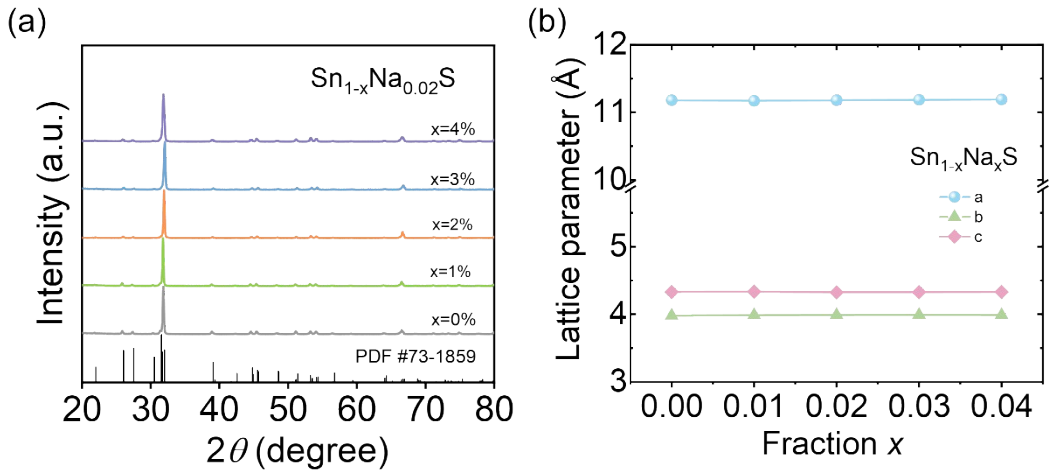

Figure S1. a) XRD powder patterns and b) Calculated lattice parameters for $Sn_{1-x}Na_xS$ (x = 0, 0.01, 0.02, 0.03, and 0.04).

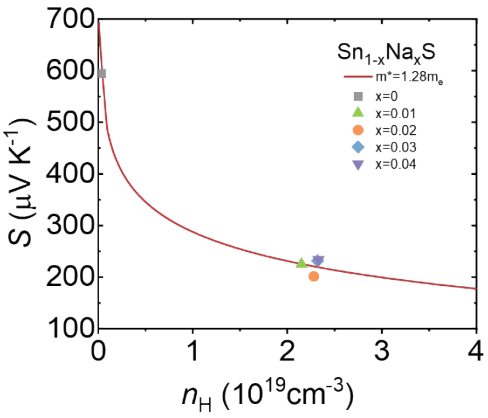

Figure S2. The relationship between S and *n* and Pisarenko line of $Sn_{1-x}Na_xS$ (x = 0, 0.01, 0.02, 0.03, and 0.04) at 300K

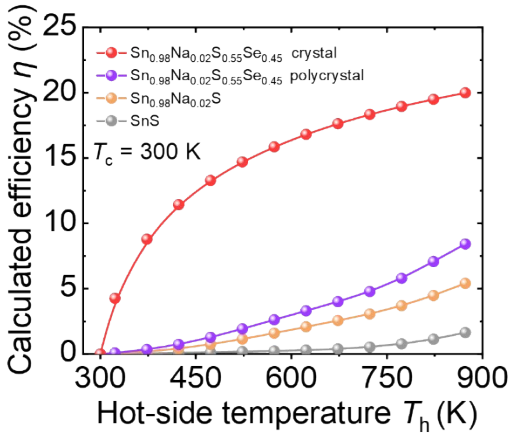

Figure S3. Theoretical efficiency of $Sn_{0.98}Na_{0.02}S_{0.55}Se_{0.45}$ crystal, $Sn_{0.98}Na_{0.02}S_{0.55}Se_{0.45}$ polycrystal, $Sn_{0.98}Na_{0.02}S$, and SnS at a cold-side temperature of 300 K.

Table S1. The carrier concentration n and carrier mobility μ of $Sn_{1-x}Na_xS$ (x = 0, 0.01, 0.02, 0.03, and 0.04) polycrystalline samples at 300 K.

Number	Sample	n_H (10^{19} cm^{-3})	μ_H (cm^2 V^{-1} s^{-1})
1	SnS	0.032	15.65
2	$Sn_{0.99}Na_{0.01}S$	2.15	6.46
3	$Sn_{0.98}Na_{0.02}S$	2.28	6.55
4	$Sn_{0.97}Na_{0.03}S$	2.32	5.15
4	$Sn_{0.96}Na_{0.04}S$	2.33	3.81

Table S2. The carrier concentration n and carrier mobility μ of $Sn_{0.98}Na_{0.02}S_{1-y}Se_y$ (y = 0, 0.1, 0.2, 0.3, 0.4, and 0.45) polycrystalline samples at 300 K.

Number	Sample	n_H (10^{19} cm^{-3})	μ_H (cm^2 V^{-1} s^{-1})
1	$Sn_{0.98}Na_{0.02}S$	2.28	6.55
2	$Sn_{0.98}Na_{0.02}S_{0.9}Se_{0.1}$	2.35	3.59
3	$Sn_{0.98}Na_{0.02}S_{0.8}Se_{0.2}$	2.42	4.08
4	$Sn_{0.98}Na_{0.02}S_{0.7}Se_{0.3}$	2.55	4.07
5	$Sn_{0.98}Na_{0.02}S_{0.6}Se_{0.4}$	2.78	4.21
6	$Sn_{0.98}Na_{0.02}S_{0.55}Se_{0.45}$	2.84	4.29

Table S3. Experimental densities for $Sn_{0.98}Na_{0.02}S_{1-y}Se_y$ (y = 0, 0.1, 0.2, 0.3, 0.4, and 0.45) polycrystalline samples.

Number	Sample	Density (g cm^{-3})
1	$Sn_{0.98}Na_{0.02}S$	4.91
2	$Sn_{0.98}Na_{0.02}S_{0.9}Se_{0.1}$	4.99
3	$Sn_{0.98}Na_{0.02}S_{0.8}Se_{0.2}$	5.17
4	$Sn_{0.98}Na_{0.02}S_{0.7}Se_{0.3}$	5.25
5	$Sn_{0.98}Na_{0.02}S_{0.6}Se_{0.4}$	5.28
6	$Sn_{0.98}Na_{0.02}S_{0.55}Se_{0.45}$	5.29

Supplementary References

[1] S. Liu, Y. Qin, Y. Wen, H. Shi, B. Qin, T. Hong, X. Gao, Q. Cao, C. Chang, L.-D. Zhao, *Adv. Funct. Mater.* 2024, **34**, 2315707.

[2] J. Callaway, H. C. von Baeyer, *Phys. Rev.* 1960, **120**, 1149-1154.

[3] H. Pang, Y. Qiu, D. Wang, Y. Qin, R. Huang, Z. Yang, X. Zhang, L.-D. Zhao, *J. Am. Chem. Soc.* 2021, **143**, 8538-8542.

[4] Y. Xiao, C. Chang, Y. Pei, D. Wu, K. Peng, *Phys. Rev. B* 2016, **94**.

[5] P. Debye, 1912.

[6] Y. Hu, S. Bai, Y. Wen, D. Liu, T. Hong, S. Liu, S. Zhan, T. Gao, P. Chen, Y. Li, *Adv. Funct. Mater.* 2025, **35**, 2414881.

[7] S. Liu, S. Bai, Y. Wen, J. Lou, Y. Jiang, Y. Zhu, D. Liu, Y. Li, H. Shi, S. Liu, *Science* 2025, **387**, 202-208.